Detection of a lipid peroxidation-induced DNA adduct across liver disease stages

Heidi Coia[1], Ning Ma[1], Aiwu Ruth He[2], Bhaskar Kallakury[3], Deborah L. Berry[2], Eva Permaul[2], Kepher H. Makambi[4], Ying Fu[2], Fung-Lung Chung[1,2]

[1]Department of Biochemistry & Molecular Biology, Georgetown University Medical Center, Washington, DC, USA; [2]Department of Oncology, [3]Department of Pathology, Lombardi Comprehensive Cancer Center, [4]Department of Biostatistics, Bioinformatics, and Biomathematics, Georgetown University, Washington, DC, USA

Contributions: (I) Conception and design: All authors; (II) Administrative support: All authors; (III) Provision of study materials or patients: All authors; (IV) Collection and assembly of data: All authors; (V) Data analysis and interpretation: H Coia, R He, B Kallakury, K Makambi, Y Fu; (VI) Manuscript writing: All authors; (VII) Final approval of manuscript: All authors.

Correspondence to: Dr. Fung-Lung Chung. E215 New Research Building, Lombardi Comprehensive Cancer Center, Georgetown University Medical Center, Washington, DC 20007, USA. Email: flc6@georgetown.edu.

Background: Oxidative stress and chronic inflammation can increase cellular levels of reactive oxygen species and lipid peroxidation (LPO) when associated with the pathogenesis of hepatocellular carcinoma (HCC), which can develop following the progression of steatosis, fibrosis and cirrhosis. Using a monoclonal antibody for cyclic γ-hydroxy-1, N^2-propanodeoxyguanosine (γ-OHPdG), a promutagenic DNA adduct formed endogenously by LPO, we examined its formation across liver disease stages to understand it's potential role in HCC development.

Methods: Formalin-fixed paraffin embedded (FFPE) liver tissue samples from 49 patients representing normal, steatosis, fibrosis, cirrhosis and HCC were stained for γ-OHPdG and 8-hydroxydeoxyguanosine (8-oxo-dG), an oxidative damage biomarker. Quantification of immunohistochemical (IHC) staining was performed using histological scoring of intensity and distribution. Using primary human hepatocytes (HH) and a stellate cell (SC) co-culture, immunocytochemical staining of γ-OHPdG and Nile Red was performed to determine if the formation of γ-OHPdG was consistent between the clinical sample disease stages and the *in vitro* steatotic and fibrotic conditions.

Results: γ-OHPdG levels varied significantly between the stages of normal and steatosis, steatosis and fibrosis, and steatosis and cirrhosis (P≤0.005). There was a trend, although not significant, of increased levels of γ-OHPdG in HCC compared to the other groups. A strong correlation was observed (Pearson's, R^2 =0.85) between levels of γ-OHPdG and 8-oxo-dG across the disease spectrum. The increase of γ-OHPdG in steatosis and decrease in fibrosis was a pattern confirmed in an *in vitro* model using primary HH co-cultured with human SCs.

Conclusions: γ-OHPdG was detected in FFPE liver tissues of patients with different stages of liver disease and *in vitro* studies, demonstrating that its formation is consistent with LPO in early stages of liver disease and suggesting that it may be a source of mutagenic DNA damage in liver disease progression.

Keywords: γ-hydroxy-1; N^2-propanodeoxyguanosine (γ-OHPdG); steatosis; fibrosis; cirrhosis; hepatocellular carcinoma (HCC)

Introduction

Hepatocellular carcinoma (HCC) is the third most common cause of cancer-related mortality worldwide (1). By the time most patients are diagnosed with HCC they have few options for palliative treatment (2,3). Most HCCs occur in cirrhotic livers, and the common mechanism for hepatocarcinogenesis is chronic inflammation associated with severe oxidative stress. Risk factors for HCC and severe oxidative stress include exposure to dietary aflatoxin B_1, cigarette smoking, and heavy drinking (4,5). Viral hepatitis (HBV, HCV) have been the prominent etiology for chronic liver inflammation. Recently the percent of individuals with chronic liver inflammation but without viral hepatitis is rising. These individuals develop chronic hepatitis from the oxidative stress resulting from fatty liver disease. Non-alcoholic fatty liver disease (NAFLD) is a very frequent condition emerging as a global health problem in recent years, with prevalence of 20–30% in the general population, and 70–90% in obese or diabetic patients; in the US, nearly 35% of the US population categorized as obese (6,7). Consequently, fatty liver disease (hepatic steatosis) has become a significant risk factor for HCC development (8). In patients with steatosis, excess accumulation of triglycerides in the liver can induce inflammation and cellular damage which is known as non-alcoholic steatohepatitis (NASH) (9,10). NASH can progress to fibrosis through recruitment of inflammatory cells into the liver tissue and production of extracellular matrix which forms the scar tissue characteristic of fibrosis (11). From fibrosis, liver disease can progress to cirrhosis, in which the liver architecture degrades and scaring is abundant. It is estimated that HCC arises from a cirrhotic liver at a rate of 2–7% every year (12). Understanding the molecular changes associated with disease risk or progression may help provide mechanistic targets for liver disease prevention.
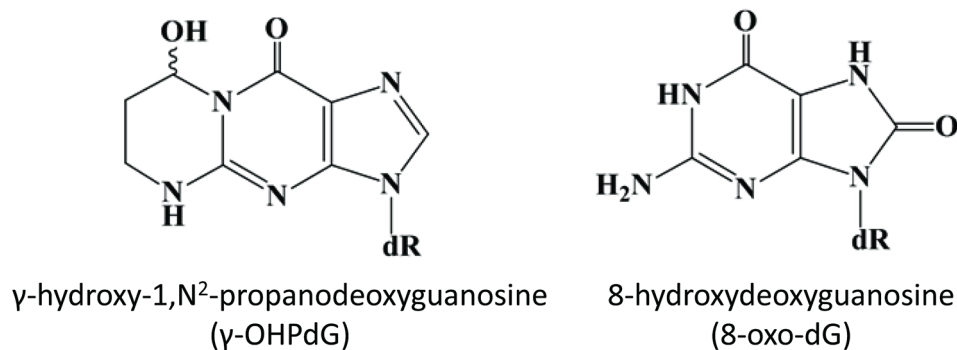
At the molecular level, inflammation in the liver induces the overproduction of free radicals which react with fatty acids (FA) in the cellular membranes forming lipid peroxides, a process known as lipid peroxidation (LPO) (13). Acrolein, an α, β-unsaturated reactive aldehyde generated by the LPO of polyunsaturated FA, forms a cyclic adduct γ-hydroxy-1, N^2-propanodeoxyguanosine (γ-OHPdG) upon binding DNA and is ubiquitously detected *in vivo* as an source of endogenous DNA damage (14-16). We have successfully developed the monoclonal antibody for immunohistochemical (IHC) detection of γ-OHPdG in human tissue and cells (17). Previously, we have shown γ-OHPdG to be an indicator of oxidative stress-induced DNA damage specifically related

to LPO (18). Levels of γ-OHPdG may also be influenced by antioxidant treatment (15). In this study, our aim is to investigate whether γ-OHPdG may have a mechanistic role in liver disease risk or severity. In the liver, chronic inflammation from obesity, alcohol consumption or viral hepatitis can cause the release of free radicals which damage DNA through LPO. γ-OHPdG is known to cause predominately G to T and G to A mutations across the genome which may potentially be involved in carcinogenesis through disruption of p53 and other critical cancer driver genes (19-22). Normally, the p53 pathway is activated to facilitate DNA repair or to induce apoptosis in tumorigenic cells, however TP53 is often mutated in initial stages of hepatocarcinogenesis (23). A spectrum of somatic mutations in HCC has identified an over-representation of G to T transversions and G to A transitions (24-26). γ-OHPdG may, therefore, play a role in hepatocarcinogenesis as it has been shown to preferentially bind to the tumor suppressor gene p53 in human cancers at the mutation hotspots found in liver cancers, including codon 249, a known location of HCC specific mutations (21,27,28). Many cellular and molecular mechanisms of hepatocarcinogenesis have been studied, however, the role of DNA damage due to chronic inflammation and obesity are still largely unknown. This study examined the relationship of γ-OHPdG with 8-hydroxydeoxyguanosine (8-oxo-dG) (*Figure 1*), a commonly used DNA damage biomarker of oxidative stress that has been shown to be mutagenic and predictive of recurrence of HCC in patients with HCV-associated solitary HCC (29-31). IHC detection of 8-oxo-dG may indicate oxidative DNA damage in tissue, however, there are no biomarkers currently used in clinical practice to predict the risk of HCC other thanserum alpha-fetoprotein levels, which are commonly used to follow the response of HCC to treatment or disease progression of HCC. The purpose of this study was to assess the potential of γ-OHPdG to serve as a specific mechanism-based prognostic indicator of DNA damage in human hepatocarcinogenesis, a possible predictor for the risk of HCC development.

Methods

Patient samples

Formalin-fixed paraffin embedded (FFPE) liver samples were obtained from 49 patients undergoing a surgery or biopsy at Medstar Georgetown University Hospital as part of their standard medical care, the tissue samples were

　　　　hbsn.amegroups.com

γ-hydroxy-1,N²-propanodeoxyguanosine
(γ-OHPdG)

8-hydroxydeoxyguanosine
(8-oxo-dG)

Figure 1 Structures of 8-hydroxydeoxyguanosine (8-oxo-dG) and γ-hydroxy-1, N²-propanodeoxyguanosine (γ-OHPdG).

Table 1 Distribution of sample characteristics

Variable	Diagnosis				
	Normal (n=9)	Steatosis (n=9)	Fibrosis (n=10)	Cirrhosis (n=10)	Hepatocellular carcinoma (n=11)
Age, mean (SD)	58.2 (±27.9)	41 (±15.3)	55.6 (±6.8)	49.8 (±8.6)	50.4 (±11.6)
Gender, n					
Male, 30	7	6	6	4	7
Female, 19	2	3	4	6	4
Race/ethnicity, n					
Black, 11	4	1	3	2	1
White, 20	1	4	6	6	3
Other/unknown, 18	4	4	1	2	7

SD, standard deviation; n, number of patients.

collected under IRB # 1992-048. Appropriate samples for the study were determined based on pathological evaluation of hematoxylin and eosin stained tissue samples by a board certified and practicing pathologist. Normal liver tissue samples were obtained from autopsy samples with no background of liver disease. Histological diagnosis designated the category of the patients as normal or one of the disease stages of steatosis, fibrosis, cirrhosis or HCC. The patients' ages ranged between 28 and 73 with an average of 52 [standard deviation (SD) ±9.7]. Characteristics of the patients from which the samples were obtained are detailed in *Table S1* of the appendix and are summarized in *Table 1*.

An additional 38 samples from patients who had a liver biopsy or curative resection of HCC as part of standard medical care, were obtained from Georgetown University Medical Center. Informed consent was obtained from all patients under IRB protocol # 1992-048. The patients had different liver pathology diagnoses, including 2 normal, 7 with cirrhosis, 3 with cirrhosis and hyperplasia, 4 with hyperplasia, and 24 with HCC.

Antibodies and immunohistochemistry

IHC staining of liver sections was performed for using antibodies for γ-OHPdG [from our laboratory (17)] and 8-oxo-dG (Trevigen, Gaithersburg, MD, USA). The FFPE samples were sectioned into five micron thick sections and de-paraffinized using xylenes and rehydrated through a graded alcohol series. Heat induced epitope retrieval was performed by immersing the tissue sections at 98 ℃ for 20 minutes in 10 mM citrate buffer (pH 6.0) with 0.05% Tween for 8-oxo-dG and with 10 mM Tris with 1 mM ethylenediaminetetraacetic acid buffer (pH 9.0)

88

Coia et al. DNA adduct formation across liver disease stages

for γ-OHPdG. IHC staining was then performed using a horseradish peroxidase-labeled polymer (Dako, Carpinteria, CA, USA) according to the instructions provided by the manufacturer. Briefly, each of the slides were treated with 3% hydrogen peroxide and 10% normal goat serum for 10 minutes, then exposed to primary antibodies for γ-OHPdG (1:500), or 8-oxo-dG, for 1 hour at room temperature as previously described (17). Slides were treated again with 3% hydrogen peroxide and then exposed to anti-mouse horseradish peroxidase-labeled polymer for 30 minutes and 3,3'-Diaminobenzidinebchromatin (Dako. Carpinteria, CA, USA) for 5 minutes. Slides were counterstained with hematoxylin (Fisher, Hampton, NH, UK), blued in 1% ammonium hydroxide, dehydrated, and mounted with acrymount embedding resin. As negative controls, consecutive sections without primary antibody were used. Images were then taken using an Olympus BX61 microscope with an attached Dp70 camera and Cellsens software system.

Histology and scoring

The intensities of γ-OHPdG and 8-oxo-dG staining were evaluated and scored for each sample. All hematoxylin and eosin slides were reviewed and semi-quantitative scoring was performed for both stains by a board certified pathologist who was blinded to all other study related data. Clinical diagnosis was confirmed prior to the blind semi-quantitative analyses of all staining. For both γ-OHPdG and 8-oxo-dG, histological scoring was obtained by adding the scores of intensity and distribution, which were assigned based on positive nuclear staining with a scale of 0–3 in each category. The intensity of nuclear staining on tumor tissue was graded as negative, weak, moderate or intense and assigned a value of 0, 1, 2, or 3, respectively. The distribution of nuclear staining was graded as negative, focal (up to 10%), regional (11% to 50%), or diffuse (>50%), depending on the percentage of positively stained nuclei. Distribution was also assigned a score based on a scale of 0 (normal) to 3 (diffuse) to make the highest additive score of up to 6 per sample when combined with the intensity score.

Stability of γ-OHPdG

To evaluate the stability of γ-OHPdG in liver tissue, serial biopsies of 20 separate cirrhotic patients were also obtained. Six cases had a substantive change in their disease status between the two biopsies (i.e., development of HCC,

development of cirrhosis, or liver transplant) and were excluded from evaluation. The remaining 14 subjects with unchanging disease status between biopsies were used for this study.

Statistical analysis

The distribution of patient characteristics was presented using frequencies and percentages for categorical data, and means and SD for numeric data. Pearson's correlation coefficients were calculated to assess the strength of the linear relationships between the five diagnosis group of γ-OHPdG and 8-oxo-dG. Independent sample t-tests were used to compare γ-OHPdG between any two of the five diagnostic groups, adjusting for multiple testing using the Bonferroni approach.

Cell culture and treatment

Primary human hepatocytes (HH) (#HUFS1M, Lot#HUM4132, Triangle Research Labs, Durham, NC, UK) were cultured in hepatocyte media (#5201, ScienCell Research Laboratories, Carlsbad, CA, USA). Triangle Research Labs provides freshly isolated HH, which undergo a proprietary isolation procedure that guarantees 96–99% purity, and only healthy and viable cells, determined through trypan blue staining, are provided. The hepatocytes were treated with FA, oleic and palmitic acid (Sigma, St. Louis) in a 2:1 ratio, respectively and dissolved in 1% bovine serum albumin in Phosphate buffered saline (PBS) for a final concentration of 1 mM. Stellate cells (SC) (#5300, ScienCell Research Laboratories, Carlsbad, CA, USA) were grown in hepatocyte media under either normal or the FA conditions described above. Conditioned media (CM) was created from FA treated HH as described (32) and FA treated HH were combined in a co-culture with the SC in a 3:1 ratio. Additional experimental controls were designed as described in supplementary methods.

Immunocytochemistry (ICC)

Following treatment, cells were fixed with 3.7% formaldehyde for 15 minutes at room temperature and washed 3 times with 1X PBS. To stain with Nile Red (Sigma, St. Louis, MO, USA), 1 μL of a 1 mg/mL stock solution was added to 10 mL of 150 mM NaCl in PBS to make a Nile Red solution. The Nile Red solution was added to the cells and incubated for 10 minutes in the dark. Following

incubation, the cells were washed 3 times with 1X PBS and stained with DAPI (Thermofisher, Waltham, MA, USA) for 4 minutes according the manufacturer recommendations. For the γ-OHPdG or alpha-smooth muscle actin (α-SMA) staining (Bethyl Laboratories, Montgomery, TX, USA), the cells were washed 3 times following fixation with 1X PBS and incubated with 0.05% tween in PBS for 5 minutes. The cells were then washed with PBS 2×5 minutes and blocked with 10% Normal Goat Serum in PBS for 1 hour. Following blocking, cells were incubated with primary antibody γ-OHPdG, or α-SMA (Bethyl Laboratories, Montgomery, TX, USA) in a 1:500 dilution in 1% bovine serum albumin (1 mL/10 mg bovine serum albumin)/PBS for 1 hour. Cells were washed with PBS 2×10 minutes and then incubated with Fluorescein-conjugated secondary antibody (Invitrogen, Carlsbad, CA, USA) in a 1:2,000 dilution in PBS for 30 minutes at RT in the dark. The cells were washed with PBS 3×5 minutes in the dark and stained with DAPI. Cells were imaged on an Olympus IX-71 Inverted Epifluorescence Microscope.

Intensity measurements

Intensity of ICC staining was measured using ImageJ (https://imagej.nih.gov/ij/). At least five fields of view were taken and analyzed for each time point. In ImageJ, images were converted into grayscale. The area measured was limited to the object (positive stained area). The threshold was adjusted to highlight the area of the cells for analysis. Integrated density of the defined area was measured and the area of the object in the entire image was quantified by the average pixel intensity. The intensity of the object is the quotient of integrated density and measured object area.

Results

IHC detection of γ-OHPdG across various liver disease stages

The 49 FFPE liver samples from patients, described in *Table 1*, were immunostained for γ-OHPdG and scored by histological evaluation as described. Positive immunostaining for γ-OHPdG was detected in each of the disease stages (*Figure 2A*). *Table S2* of the appendix details the quantification of positive staining for normal tissue and the subsequent disease stages. Quantification of the levels of staining, based on histological scoring in normal tissue had a mean score of 1.9 for γ-OHPdG. The average scores

were the highest in steatosis samples with a mean score of 3.4 for γ-OHPdG, showing a significant increase (P≤0.005) from the normal samples. This suggests that the increased LPO-induced DNA damage, consistent with the onset of fatty liver in steatosis, may represent a crucial pathologic event during an early stage of hepatocarcinogenesis. The lowest average score was obtained from the fibrosis samples (mean =0.8). The decrease in γ-OHPdG levels were highly significant between the stages of steatosis and fibrosis (P=0.0009), illustrated in *Figure 2B*. A highly significant difference between steatosis and cirrhosis for γ-OHPdG was also observed (P=0.0009). The overall γ-OHPdG profile during the disease stages leading to hepatocarcinogenesis consists of an initial peak in steatosis, followed by a significant decrease in fibrosis and cirrhosis, and then an increase in HCC. However, there is a wide range of γ-OHPdG levels observed among individual fibrosis, cirrhosis and HCC samples, including some with relative high levels as well as non-detectible levels of γ-OHPdG.

IHC detection of 8-oxo-dG across various liver disease stages

Adjacent sections from the same 49 FFPE human livers as described above were immunostained for 8-oxo-dG. Similar to the immunostaining for γ-OHPdG, 8-oxo-dG was detected in each of the disease stages (*Figure 2A*). *Table S2* of the appendix shows the specific quantification of positive staining for 8-oxo-dG as compared to γ-OHPdG in normal tissues and the subsequent disease stages. Quantification of the IHC staining in normal tissues, based on histological scoring, had a mean of 0.6 for 8-oxo-dG. Analogous to that of γ-OHPdG, average scores were the highest in steatosis samples, showing a significant increase (P≤0.005) from normal samples with a mean score of 2.8 and the lowest average score (0.4) was obtained from the fibrosis samples (*Figure 2C*). Additional control experiments performed under separate culture conditions using HH and SC showed that through staining, imaging, and intensity quantification, the results discussed above were not related to other independent variables (supplementary results).

Correlation between γ-OHPdG and 8-oxo-dG levels in human liver samples

γ-OHPdG and 8-oxo-dG levels were compared using Pearson's correlation, which was run using the average sample scores across all disease stage groups. The
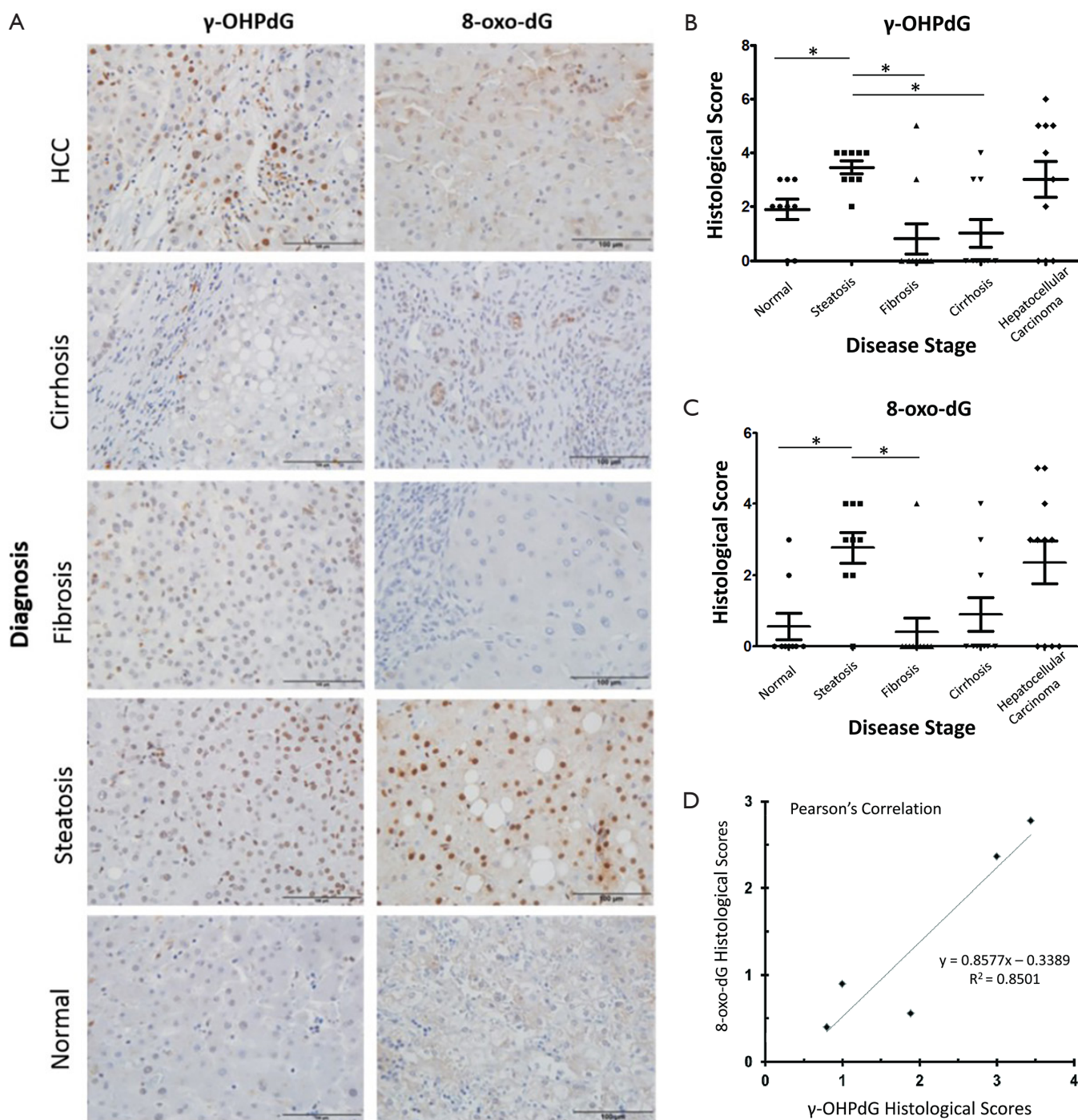
Figure 2 Detection and scoring of γ-OHPdG and 8-oxo-dG in FFPE human liver tissues in different stages of diagnosis. (A) Representative IHC staining of FFPE human liver tissue sections positive for γ-OHPdG or 8-oxo-dG. Scale bar indicates 100 μm; (B) dot plots of γ-OHPdG and (C) 8-oxo-dG levels based on histological scoring across the disease spectrum, center line indicates mean and whiskers standard error of the mean (SEM). * indicates significance (P≤0.005) between groups using two-sample independent *t*-tests; (D) histological score quantification across groups with Pearson's correlation between γ-OHPdG and 8-oxo-dG, Pearson's R^2 =0.85. The symbols (triangle/circular/square/diamond) are for each individual histology score per sample in each group. FFPE, formalin-fixed paraffin embedded; IHC, immunohistochemical.

Table 2 Stability of γ-OHPdG based on histological score in 14 patients with serial liver biopsies separated by the time in weeks indicated

Sample information	P1	P2	P3	P4	P5	P6	P7	P8	P9	P10	P11	P12	P13	P14
Weeks between biopsies	3.3	3.3	8.6	9.4	21.7	30.9	32.7	57.3	64	69.4	70.1	89.6	107.7	159.1
Biopsy 1 score	0	3	0	2	3	4	0	1	3	5	0	2	0	2
Biopsy 2 score	2	3	2	2	3	3	0	2	3	5	0	2	0	2

P, patient.

correlation across the five pairs of diagnosis types according to histological score was strong (R^2 =0.85) as shown in *Figure 2D*. A strong correlation suggests that the formation of γ-OHPdG, as expected, is related to oxidative damage. Similarly, when the individual additive histological scores of intensity and distribution for each patient, regardless of disease stage, were compared between γ-OHPdG and 8-oxo-dG, there was also a strong and significant correlation (R^2 =0.63) (the calculation are available in the appendix, *Table S3*).

Complementary sample set

To further examine the levels of γ-OHPdG in different liver disease stages, a separate set of 38 samples was obtained from patients who had a liver biopsy or curative resection of HCC with the pathology diagnoses of normal, cirrhosis, cirrhosis with hyperplasia, hyperplasia or HCC. Again, there was a significant association (P=0.0364) between pathology and immunoscore of γ-OHPdG (see supplementary table of scores in the appendix, *Table S4*). The samples with the highest scores for γ-OHPdG were found in the HCC group, while cirrhotic patients were more likely to have a lower score.

Stability of γ-OHPdG in serial biopsies

Cirrhosis is a critical link between liver disease and HCC. Late stage cirrhosis is irreversible and is an underlying condition in the majority of HCC cases (33). In order to evaluate γ-OHPdG as a clinical indicator of specific DNA damage by LPO for liver diseases, its stability in liver tissue was studied in serial liver biopsies of 14 cirrhotic patients. The interval between the serial biopsies ranged from 3.3 to 159 weeks. All 14 subjects remained in either the low (2 or less) or the high (3 or more) IHC score category (i.e., there was no crossing over from low to high or high to low in the interval between the 2 biopsies) (*Table 2*). These results indicate that the levels of γ-OHPdG in the liver remain stable in individual cirrhotic patients.

γ-OHPdG detection in cultured primary human liver cells

In order to better study the mechanism of γ-OHPdG formation in liver disease, a cell model was developed to study the formation of γ-OHPdG in the transition from steatosis to fibrosis. A model has previously been developed which demonstrated that SC could become activated and display fibrogenic traits following treatment with CM from steatotic hepatocytes (32). In this study, FA treated HH increasingly accumulated lipids over the course of 5 days of treatment as indicated by the lipophilic stain, Nile Red (*Figure 3A*). Similarly, the FA treatment increased the formation of γ-OHPdG over this time course (*Figure 3B*). SC incubated with CM grown in a co-culture with FA-treated hepatocytes over 3 days showed fibrogenic activation of the SC, as indicated by α-SMA staining (*Figure 4A*). These co-culture conditions also resulted in reduction of γ-OHPdG compared to FA-treated hepatocytes alone (*Figure 4B*). As controls, other conditions of this model were tested to ensure that the observed effects were not a result of the co-culture alone or exposure of the cells to alternate conditions of fatty acid and normal media (see supplementary figures describing culture conditions and results in *Figures S1-S4*).

Discussion

Chronic inflammation and its associated LPO increase the risk of cancer (34,35). LPO-derived DNA adducts may, therefore, serve as indicators of disease etiology. γ-OHPdG, a promutagenic DNA lesion derived from acrolein as a secondary product of LPO, has been implicated in cancer development (19,20,22,36). Acrolein cannot only react with DNA to form γ-OHPdG, but can also inhibit DNA repair, enhancing the probability for mutations (37). In this study we examined γ-OHPdG in
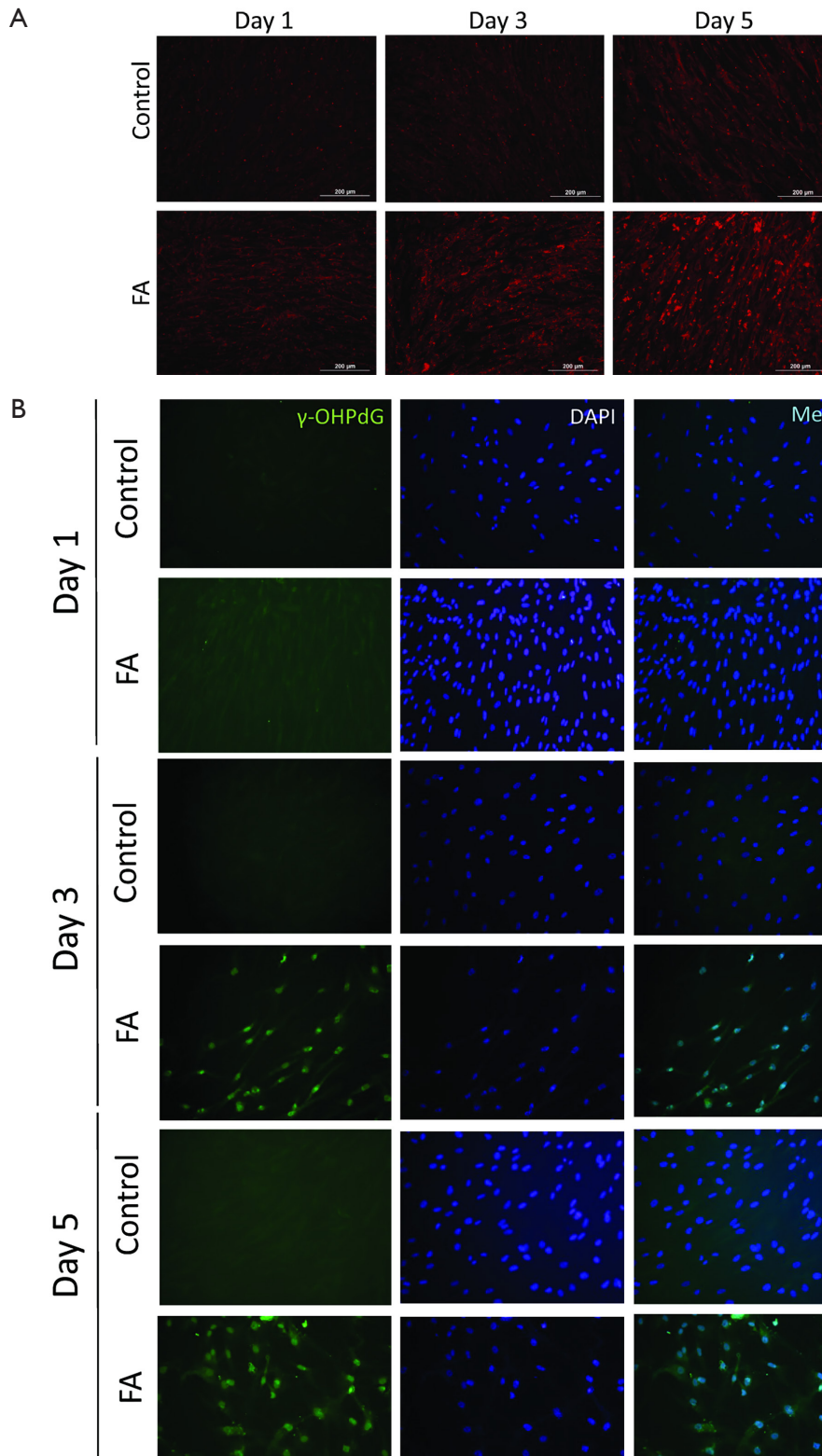
Figure 3 ICC of FA treated HH (20× magnification). (A) FA-treated HH stained with Nile Red following treatment after 1, 3 and 5 days. Scale bar indicates 200 μm; (B) γ-OHPdG staining of FA treated HH after 1, 3 and 5 days. ICC, immunocytochemistry; FA, fatty acids; HH, human hepatocytes.

hbsn.amegroups.com
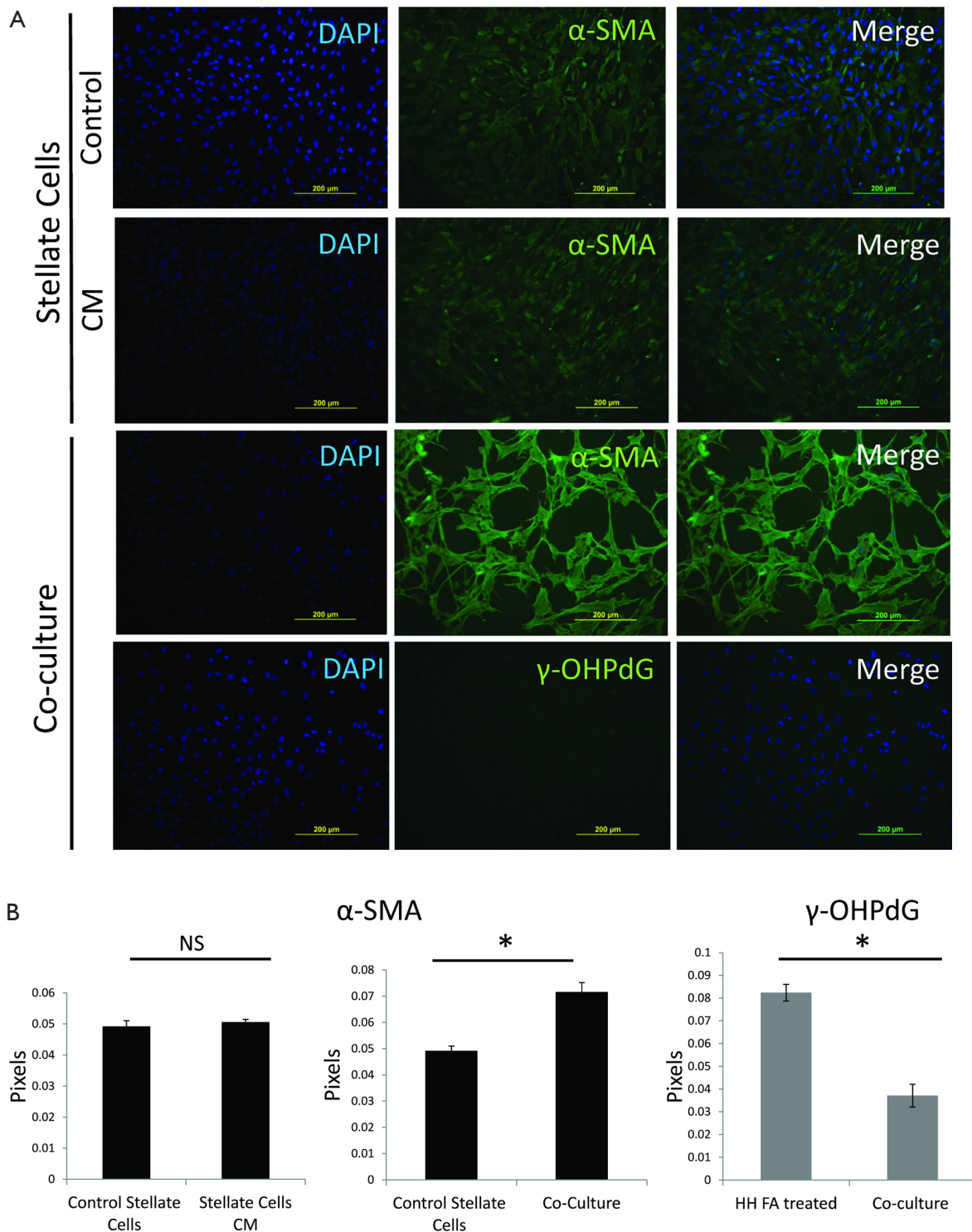
Figure 4 ICC and intensity quantification of α-SMA and γ-OHPdG in SC and under co-culture conditions. (A) SC untreated and treated with CM for 3 days stained for α-SMA and co-culture for 3 days, stained for α-SMA and γ-OHPdG (20× magnification, scale bar indicates 200 µm); (B) quantification of the staining intensity of α-SMA and γ-OHPdG of the SC and HH before and during co-culture conditions. * indicates significance (P≤0.005) between groups using two-sample independent *t*-tests. NS indicates not significant. ICC, immunocytochemistry; SC, stellate cell; CM, conditioned media; α-SMA, alpha-smooth muscle actin; HH, human hepatocytes.

hbsn.amegroups.com   *HepatoBiliary Surg Nutr* 2018;7(2):85-97

94

Coia et al. DNA adduct formation across liver disease stages

human liver samples representing normal tissue and the disease stages of steatosis, fibrosis, cirrhosis and HCC and have found evidence that may support its association with hepatocarcinogenesis.

γ-OHPdG was detected in FFPE human liver tissue samples by IHC staining using the monoclonal antibody that we previously developed (17,38,39). In the present study, we showed that γ-OHPdG levels varied greatly in patients with different stages of liver disease during the progression of HCC. The highest levels occurred during steatosis, where inflammation is the primary response to excess lipid accumulation in hepatocytes which stimulates LPO and impairs DNA repair (37,40). It is conceivable that as γ-OHPdG accumulates in the liver during steatosis there is a greater chance of mutations in the form of G > T transversions. This event may be exacerbated in fibrosis and cirrhosis by compensatory growth which occurs with liver injury. γ-OHPdG could serve as an early biomarker for HCC in which the free radicals generated by inflammation have been shown to act cooperatively during p53 regulated tumorigenesis (41). Cirrhosis is the major risk factor for HCC; up to 15% of cirrhosis cases per year advance to HCC depending on the associated genetic and environmental risk factors (42,43). HCC is the most common cause of lethality in cirrhosis patients despite the etiology of the disease (44). In autopsies of individuals who succumbed to HCC, 80–90% had underlying cirrhosis (33). It is possible that the high levels of γ-OHPdG, particularly in a few of those patients with cirrhosis we have identified, may predict an increased risk of HCC. This notion, however, needs to be verified through future investigations which include a larger cohort of patients. The consistency in the score of cirrhotic patients over time however, suggests that γ-OHPdG levels are not influenced by other factors and the underlying level may be a predictor of patients at high risk of progressing to HCC.

The increase of γ-OHPdG in steatosis was followed by a dramatic decrease in fibrosis and cirrhosis. While the mechanisms behind the apparent drop of γ-OHPdG in these stages are unclear, the induction of apoptosis as a result of elevated DNA damage may play a role (45). Furthermore, decreased fat content in the liver following steatosis, where the effects of LPO from fat accumulation are conceivably the most severe, might be another factor that contributes to the decreased levels of γ-OHPdG. Oxidative stress contributes to the progression of liver disease regardless of etiology (46). The levels of DNA damage in each stage of liver disease may vary depending on the efficiency of DNA repair, cell proliferation and apoptosis (47). *In vitro*

treatment of human liver cells (HepG2, Huh7, WRL68) with oleic a palmitic FA which are commonly found in the diet, leads to increased lipid intake, fat accumulation and an inflammatory and fibrogenic response similar to what is seen in liver disease progression (48-50). These models have helped characterize the molecular events that lead to the symptoms of NAFLD and NASH. In our study, the change in γ-OHPdG levels were replicated in a co-culture of HH and SC, treated with FA. FA treated HH represented steatosis-like conditions and the co-culture displayed fibrotic-like conditions, such as activation of the SC, where γ-OHPdG levels were reduced compared to steatotic HH cells and CM-treated SC alone. This trend was consistent with the γ-OHPdG changes observed in the clinical samples between the stages of steatosis and fibrosis, which appear to validate the cellular changes that occur between lipid accumulation in steatosis and fibrotic activation in fibrosis in relation to γ-OHPdG formation.

8-Oxo-dG is a widely studied marker of oxidative DNA damage related to inflammation and tumorigenesis (29,31). Our data showing the strong correlation between of γ-OHPdG and 8-oxo-dG in both the disease groups and individual patients suggests a strong mechanistic link between the two markers. To our best knowledge, this is first study to demonstrate the relationship of 8-oxo-dG and γ-OHPdG during liver cancer development. In an earlier study by Kitada T *et al.*, IHC staining of liver tissues from patients with chronic liver disease showed that the number of 8-oxo-dG-positive hepatocytes was significantly correlated with chronic hepatitis disease severity, suggesting chronic inflammation is important in hepatocarcinogenesis (51). We found, however, fibrosis consistently had the lowest levels of 8-oxo-dG and γ-OHPdG (*Figure 2B,C*). In a separate set of 38 samples consisting of normal, cirrhosis, cirrhosis and hyperplasia and hyperplasia with HCC, a significant association was also found between liver disease severity and the immunoscore of γ-OHPdG. This demonstrates that γ-OHPdG levels are lower in cirrhosis and normal tissue compared to HCC and that γ-OHPdG may serve as an indicator of the DNA damage which may lead to hepatocarcinogenesis. An increase of γ-OHPdG was noted in most HCC samples, indicative of oxidative stress, which is commonly elevated in tumors compared to normal, fibrosis and cirrhosis (52). Our data also showed some significant individual variability in γ-OHPdG levels within each disease stage (*Figure 2A,B*), but they remained stable in serial biopsies of individual patients (*Table 2*). The variation of γ-OHPdG levels within stages is especially notable in

cirrhosis and HCC patients. Additional longitudinal studies that can incorporate prior and current treatment as well as the clinical outcomes of patients would provide insight into explaining these results and how these differences may be used to predict disease risk.

1,N^6-ethenodeoxyadenosine (εdA), a related LPO-derived cyclic DNA adduct has been investigated for its role in hepatocarcinogenesis (53,54) . Results of these studies showed that a gradual accumulation of εdA occurs in diseased livers during HCC development, suggesting that it may contribute to mutations. The formation of the etheno adduct in liver cancer shown by these studies also point to the role of lipid accumulation in the liver and the oxidative stress associated with chronic inflammation as its source (55). However, unlike εdA, γ-OHPdG levels have been found to correlate with 8-oxo-dG and increase sharply in steatosis compared to that in normal livers, rendering it potentially useful in monitoring HCC development and understanding its specific role in the process of hepatocarcinogenesis.

There are many factors to be considered for γ-OHPdG to be used in clinical investigations, including the variations in the source and pathology of tissue, effects of the disease or treatment, study sample size, and time period and method of sample collection (14). DNA damage caused by formalin fixation of tissue may make it difficult to discern γ-OHPdG specific damage in some samples, particularly in biopsies which have a small surface area. The IHC method described in this study is more amenable for the detection of γ-OHPdG in clinical samples than the previously developed high-performance liquid chromatography-tandem mass spectrometry method which requires relatively high amounts of frozen tissue (500 mg or more) for detection (56-58). The antibody-based IHC method provides a sensitive, practical, and cost effective way to efficiently monitor this adduct in liver tissue. As its levels are the highest in steatosis, γ-OHPdG, could be used as a biomarker in the pathogenesis of NASH, the early stages of which are currently difficult to distinguish (59). Establishing γ-OHPdG as a clinical prognostic biomarker will require further method development for its detection in blood or urine. The levels of excreted γ-OHPdG and 8-oxo-dG may indicate the extent of DNA repair that occurs across the liver disease spectrum. The excreted level of γ-OHPdG combined with the background levels in liver tissue, may, therefore, determine the extent of oxidative-related DNA damage that is related to γ-OHPdG. While our studies have shown a potential relationship of γ-OHPdG in HCC development, future clinical studies will be needed to examine its validity to monitor patients with a high risk for HCC for better prevention and treatment.

Acknowledgements

Footnote

Conflicts of Interest: The authors have no conflicts of interest to declare.

Ethical Statement: The study was approved by the institutional review board of Georgetown University Medical Center (No. 1992-048) and informed consent was obtained from all patients.

References

1. Jemal A, Bray F, Center MM, et al. Global cancer statistics. CA Cancer J Clin 2011;61:69-90.
2. Venook AP, Papandreou C, Furuse J, et al. The incidence and epidemiology of hepatocellular carcinoma: a global and regional perspective. Oncologist 2010;15 Suppl 4:5-13.
3. Bialecki ES, Di Bisceglie AM. Diagnosis of hepatocellular carcinoma. HPB (Oxford) 2005;7:26-34.
4. Flores A, Marrero JA. Emerging trends in hepatocellular carcinoma: focus on diagnosis and therapeutics. Clin Med Insights Oncol 2014;8:71-6.
5. Karin M, Greten FR. NF-kappaB: linking inflammation and immunity to cancer development and progression. Nat Rev Immunol 2005;5:749-59.
6. Vernon G, Baranova A, Younossi ZM. Systematic review: the epidemiology and natural history of non-alcoholic fatty liver disease and non-alcoholic steatohepatitis in adults. Aliment Pharmacol Ther 2011;34:274-85.
7. Ogden CL, Carroll MD, Kit BK, et al. Prevalence of childhood and adult obesity in the United States, 2011-2012. JAMA 2014;311:806-14.
8. Sun B, Karin M. Obesity, inflammation, and liver cancer. J Hepatol 2012;56:704-13.
9. Sakaguchi S, Takahashi S, Sasaki T, et al. Progression of Alcoholic and Non-alcoholic Steatohepatitis: Common Metabolic Aspects of Innate Immune System and Oxidative

Stress. Drug Metab Pharmacokinet 2011;26:30-46.

10. Matteoni CA, Younossi ZM, Gramlich T, et al. Nonalcoholic fatty liver disease: a spectrum of clinical and pathological severity. Gastroenterology 1999;116:1413-9.

11. Bataller R, Brenner DA. Liver fibrosis. J Clin Invest 2005;115:209-18.

12. Michelotti GA, Machado MV, Diehl AM. NAFLD, NASH and liver cancer. Nat Rev Gastroenterol Hepatol 2013;10:656-65.

13. Girotti AW. Lipid hydroperoxide generation, turnover, and effector action in biological systems. J Lipid Res 1998;39:1529-42.

14. Nair U, Bartsch H, Nair J. Lipid peroxidation-induced DNA damage in cancer-prone inflammatory diseases: a review of published adduct types and levels in humans. Free Radic Biol Med 2007;43:1109-20.

15. Fu Y, Nath RG, Dyba M, et al. In vivo detection of a novel endogenous etheno-DNA adduct derived from arachidonic acid and the effects of antioxidants on its formation. Free Radic Biol Med 2014;73:12-20.

16. Nath RG, Chung FL. Detection of exocyclic 1,N2-propanodeoxyguanosine adducts as common DNA lesions in rodents and humans. Proc Natl Acad Sci U S A 1994;91:7491-5.

17. Pan J, Awoyemi B, Xuan Z, et al. Detection of acrolein-derived cyclic DNA adducts in human cells by monoclonal antibodies. Chem Res Toxicol 2012;25:2788-95.

18. Chung FL, Chen HJ, Nath RG. Lipid peroxidation as a potential endogenous source for the formation of exocyclic DNA adducts. Carcinogenesis 1996;17:2105-11.

19. Yang IY, Chan G, Miller H, et al. Mutagenesis by acrolein-derived propanodeoxyguanosine adducts in human cells. Biochemistry 2002;41:13826-32.

20. VanderVeen LA, Hashim MF, Nechev LV, et al. Evaluation of the mutagenic potential of the principal DNA adduct of acrolein. J Biol Chem 2001;276:9066-70.

21. Choudhury S, Dyba M, Pan J, et al. Repair kinetics of acrolein- and (E)-4-hydroxy-2-nonenal-derived DNA adducts in human colon cell extracts. Mutat Res 2013;751-2:15-23.

22. Feng Z, Hu W, Hu Y, et al. Acrolein is a major cigarette-related lung cancer agent: Preferential binding at p53 mutational hotspots and inhibition of DNA repair. Proc Natl Acad Sci U S A 2006;103:15404-9.

23. Hussain SP, Schwank J, Staib F, et al. TP53 mutations and hepatocellular carcinoma: insights into the etiology and pathogenesis of liver cancer. Oncogene 2007;26:2166-76.

24. Fujimoto A, Totoki Y, Abe T, et al. Whole-genome sequencing of liver cancers identifies etiological influences on mutation patterns and recurrent mutations in chromatin regulators. Nat Genet 2012;44:760-4.

25. Guichard C, Amaddeo G, Imbeaud S, et al. Integrated analysis of somatic mutations and focal copy-number changes identifies key genes and pathways in hepatocellular carcinoma. Nature Genetics 2012;44:694-U120.

26. Feitelson MA, Sun B, Satiroglu Tufan NL, et al. Genetic mechanisms of hepatocarcinogenesis. Oncogene 2002;21:2593-604.

27. Wang HT, Zhang S, Hu Y, et al. Mutagenicity and sequence specificity of acrolein-DNA adducts. Chem Res Toxicol 2009;22:511-7.

28. Wang HT, Weng MW, Chen WC, et al. Effect of CpG methylation at different sequence context on acrolein- and BPDE-DNA binding and mutagenesis. Carcinogenesis 2013;34:220-7.

29. Shibutani S, Takeshita M, Grollman AP. Insertion of Specific Bases during DNA-Synthesis Past the Oxidation-Damaged Base 8-Oxodg. Nature 1991;349:431-4.

30. Maki A, Kono H, Gupta M, et al. Predictive power of biomarkers of oxidative stress and inflammation in patients with hepatitis C virus-associated hepatocellular carcinoma. Ann Surg Oncol 2007;14:1182-90.

31. Kasai H. Analysis of a form of oxidative DNA damage, 8-hydroxy-2'-deoxyguanosine, as a marker of cellular oxidative stress during carcinogenesis. Mutat Res 1997;387:147-63.

32. Wobser H, Dorn C, Weiss TS, et al. Lipid accumulation in hepatocytes induces fibrogenic activation of hepatic stellate cells. Cell Res 2009;19:996-1005.

33. Simonetti RG, Camma C, Fiorello F, et al. Hepatocellular carcinoma. A worldwide problem and the major risk factors. Dig Dis Sci 1991;36:962-72.

34. Setshedi M, Wands JR, Monte SM. Acetaldehyde adducts in alcoholic liver disease. Oxid Med Cell Longev 2010;3:178-85.

35. Bartsch H, Nair J. Oxidative stress and lipid peroxidation-derived DNA-lesions in inflammation driven carcinogenesis. Cancer Detect Prev 2004;28:385-91.

36. Nath RG, Ocando JE, Guttenplan JB, et al. 1,N2-propanodeoxyguanosine adducts: potential new biomarkers of smoking-induced DNA damage in human oral tissue. Cancer Res 1998;58:581-4.

37. Wang HT, Hu Y, Tong D, et al. Effect of carcinogenic acrolein on DNA repair and mutagenic susceptibility. J Biol Chem 2012;287:12379-86.

38. Greenspan EJ, Lee H, Dyba M, et al. High-throughput,

quantitative analysis of acrolein-derived DNA adducts in human oral cells by immunohistochemistry. J Histochem Cytochem 2012;60:844-53.

39. Pan J, Awoyemi B, Xuan ZL, et al. Detection of Acrolein-Derived Cyclic DNA Adducts in Human Cells by Monoclonal Antibodies. Chem Res Toxicol 2012;25:2788-95.

40. Seki S, Kitada T, Yamada T, et al. In situ detection of lipid peroxidation and oxidative DNA damage in non-alcoholic fatty liver diseases. J Hepatol 2002;37:56-62.

41. Stauffer JK, Scarzello AJ, Jiang Q, et al. Chronic inflammation, immune escape, and oncogenesis in the liver: a unique neighborhood for novel intersections. Hepatology 2012;56:1567-74.

42. Teufel A, Weinmann A, Centner C, et al. Hepatocellular carcinoma in patients with autoimmune hepatitis. World J Gastroenterol 2009;15:578-82.

43. Guzman G, Brunt EM, Petrovic LM, et al. Does nonalcoholic fatty liver disease predispose patients to hepatocellular carcinoma in the absence of cirrhosis? Arch Pathol Lab Med 2008;132:1761-6.

44. Sanyal AJ, Yoon SK, Lencioni R. The etiology of hepatocellular carcinoma and consequences for treatment. Oncologist 2010;15 Suppl 4:14-22.

45. Pan J, Keffer J, Emami A, et al. Acrolein-derived DNA adduct formation in human colon cancer cells: its role in apoptosis induction by docosahexaenoic acid. Chem Res Toxicol 2009;22:798-806.

46. Cichoz-Lach H, Michalak A. Oxidative stress as a crucial factor in liver diseases. World J Gastroenterol 2014;20:8082-91.

47. Guicciardi ME, Gores GJ. Apoptosis: a mechanism of acute and chronic liver injury. Gut 2005;54:1024-33.

48. Gomez-Lechon MJ, Donato MT, Martinez-Romero A, et al. A human hepatocellular in vitro model to investigate steatosis. Chem Biol Interact 2007;165:106-16.

49. Cui W, Chen SL, Hu KQ. Quantification and mechanisms of oleic acid-induced steatosis in HepG2 cells. Am J Transl Res 2010;2:95-104.

50. Ricchi M, Odoardi MR, Carulli L, et al. Differential effect of oleic and palmitic acid on lipid accumulation and apoptosis in cultured hepatocytes. J Gastroenterol Hepatol 2009;24:830-40.

51. Kitada T, Seki S, Iwai S, et al. In situ detection of oxidative DNA damage, 8-hydroxydeoxyguanosine, in chronic human liver disease. J Hepatol 2001;35:613-8.

52. Halliwell B. Oxidative stress and cancer: have we moved forward? Biochem J 2007;401:1-11.

53. Frank A, Seitz HK, Bartsch H, et al. Immunohistochemical detection of 1,N-6-ethenodeoxyadenosine in nuclei of human liver affected by diseases predisposing to hepato-carcinogenesis. Carcinogenesis 2004;25:1027-31.

54. Zhou L, Yang YZ, Tian DA, et al. Oxidative stress-induced 1, N-6-ethenodeoxyadenosine adduct formation contributes to hepatocarcinogenesis. Oncol Rep 2013;29:875-84.

55. Cohen JC, Horton JD, Hobbs HH. Human Fatty Liver Disease: Old Questions and New Insights. Science 2011;332:1519-23.

56. Chung FL, Wu MY, Basudan A, et al. Regioselective Formation of Acrolein-Derived Cyclic 1,N-2-Propanodeoxyguanosine Adducts Mediated by Amino Acids, Proteins, and Cell Lysates. Chem Res Toxicol 2012;25:1921-8.

57. Taghizadeh K, McFaline JL, Pang B, et al. Quantification of DNA damage products resulting from deamination, oxidation and reaction with products of lipid peroxidation by liquid chromatography isotope dilution tandem mass spectrometry. Nat Protoc 2008;3:1287-98.

58. Zhang S, Villalta PW, Wang M, et al. Detection and quantitation of acrolein-derived 1,N2-propanodeoxyguanosine adducts in human lung by liquid chromatography-electrospray ionization-tandem mass spectrometry. Chem Res Toxicol 2007;20:565-71.

59. Farrell GC, Larter CZ. Nonalcoholic fatty liver disease: from steatosis to cirrhosis. Hepatology 2006;43:S99-S112.

Supplementary methods

In order to confirm the effects of the co-culture conditions on stellate cells and HH, various conditions were created to test the cellular response related to γ-OHPdG formation and fibrogenic activation as indicated by α-SMA. Staining, imaging and intensity quantification was performed as described in the Methods section of this manuscript. Figure S1 is a diagram of the conditions that were tested. In brief, HH were grown in either normal or FA media and then co-cultured with stellate cells in either normal media or FA media. Stellate cells were grown independent of co-culture conditions in normal media and FA media to determine their α-SMA levels. Images were taken using an Olympus IX-71 Inverted Epifluorescence Microscope.

Results

The intensity γ-OHPdG staining was measured from HH cultured for 3 days in normal or FA media and there was a significant increase in staining intensity of γ-OHPdG in the FA-treated HH by day 3 (*Figure S2A*). When the FA HH were co-cultured with SC in either FA media or normal media, γ-OHPdG levels decreased compared to FA treated HH alone (*Figure S2A*). SC's grown in either FA media or normal media for 3 days resulted in increased α-SMA staining intensity over time in the FA media and significantly lower than normal at day 1, but higher by day 3 (*Figure S3A,B*). Lastly, there was no difference in α-SMA between normal HH co-cultured with normal SC grown in normal media and FA HH co-cultured with FA SC in normal media or FA HH co-cultured with FA SC in FA media (*Figure S4A,B*) showing that the co-culture conditions described in the main manuscript are required for fibrogenic activation and decreased γ-OHPdG formation.

Table S1 Individual sample information for FFPE liver tissue

Age	Race	Gender	Diagnosis	γ-OHPdG			8-OHdG		
				Intensity	Distribution	Total score	Intensity	Distribution	Total score
87	Black/African American	Female	Normal	2	1	3	2	1	3
0	Unknown	Female	Normal	0	0	0	0	0	0
68	Black/African American	Male	Normal	1	1	2	1	1	2
70	Black/African American	Male	Normal	1	1	2	0	0	0
64	White/Caucasian	Male	Normal	2	1	3	0	0	0
36	Black/African American	Male	Normal	2	1	3	0	0	0
44	Unknown	Male	Normal	1	1	2	0	0	0
54	Unknown	Male	Normal	1	1	2	0	0	0
101	Unknown	Male	Normal	0	0	0	0	0	0
22	Black/African American	Female	Steatosis	1	2	3	1	3	4
39	Unknown	Male	Steatosis	2	2	4	2	1	3
52	Unknown	Female	Steatosis	2	1	3	1	1	2
101	Unknown	Male	Steatosis	1	2	3	1	1	2
58	White/Caucasian	Male	Steatosis	1	1	2	0	0	0
44	White/Caucasian	Female	Steatosis	2	2	4	2	1	3
45	White/Caucasian	Male	Steatosis	2	2	4	2	2	4
61	Other	Male	Steatosis	2	2	4	2	1	3
40	White/Caucasian	Male	Steatosis	2	2	4	2	2	4
58	White/Caucasian	Male	Fibrosis	0	0	0	0	0	0
48	White/Caucasian	Female	Fibrosis	0	0	0	0	0	0
48	Black/African American	Female	Fibrosis	0	0	0	0	0	0
56	White/Caucasian	Female	Fibrosis	0	0	0	0	0	0
56	Unknown	Male	Fibrosis	0	0	0	0	0	0
46	Black/African American	Male	Fibrosis	0	0	0	0	0	0
54	White/Caucasian	Male	Fibrosis	3	2	5	3	1	4
61	White/Caucasian	Male	Fibrosis	0	0	0	0	0	0
70	Black/African American	Female	Fibrosis	0	0	0	0	0	0
59	White/Caucasian	Male	Fibrosis	2	1	3	0	0	0
45	White/Caucasian	Male	Cirrhosis	0	0	0	0	0	0
45	Unknown	Female	Cirrhosis	0	0	0	0	0	0
38	Black/African American	Female	Cirrhosis	2	2	4	2	2	4
52	Black/African American	Female	Cirrhosis	2	1	3	0	0	0
58	White/Caucasian	Female	Cirrhosis	0	0	0	0	0	0
57	White/Caucasian	Male	Cirrhosis	0	0	0	0	0	0
54	White/Caucasian	Female	Cirrhosis	0	0	0	0	0	0
58	White/Caucasian	Female	Cirrhosis	0	0	0	1	1	2
33	Unknown	Male	Cirrhosis	2	1	3	2	1	3
58	White/Caucasian	Male	Cirrhosis	0	0	0	0	0	0
53	Unknown	Female	HCC	2	1	3	2	1	3
39	Unknown	Male	HCC	3	2	5	2	1	3
73	White/Caucasian	Male	HCC	1	2	3	3	2	5
67	Unknown	Male	HCC	0	0	0	0	0	0
51	Unknown	Male	HCC	0	0	0	0	0	0
46	Black/African American	Female	HCC	3	2	5	1	2	3
50	White/Caucasian	Female	HCC	3	3	6	3	2	5
47	White/Caucasian	Male	HCC	1	1	2	0	0	0
54	Unknown	Male	HCC	3	2	5	2	1	3
46	Unknown	Male	HCC	0	0	0	0	0	0
28	Unknown	Female	HCC	1	3	4	2	2	4

Intensity score: negative =0, weak =1, moderate =2, intense =3; distribution score: negative =0, focal =1, regional =2, diffused =3. FFPE, formalin-fixed paraffin embedded; HCC, hepatocellular carcinoma.

Table S2 Histological score assessment for γ-OHPdG and 8-OHdG in livers obtained at different stages of disease

Diagnosis	Mean score (SD)		Number positive cases/total number (%)	
	γ-OHPdG	8-OHdG	γ-OHPdG	8-OHdG
Normal	1.9 (±1.1)	0.6 (±1.1)	7/9 [78]	2/9 [22]
Steatosis	3.4 (±0.7)	2.8 (±1.2)	9/9 [100]	8/9 [89]
Fibrosis	0.8 (±1.7)	0.4 (±1.2)	2/10 [20]	2/10 [20]
Cirrhosis	1.0 (±1.5)	0.9 (±1.4)	3/10 [30]	3/10 [30]
Carcinoma	3.0 (±2.1)	2.4 (±2.0)	8/11 [73]	7/11 [64]

Table S3 Pearson's correlation of patients' individual scores between γ-OHPdG and 8-oxo-dG

| Factor	Value
Number of γ-OHPdG and 8-oxo-dG Pairs	49
Pearson r	0.80
P value (two-tailed)	<0.0001
R squared	0.63

For *Table S3*, a non-parametric Pearson's correlation was performed (GraphPad Prism version 6.00 for Windows, GraphPad Software, La Jolla California USA, www.graphpad.com) using the total score for each patient between γ-OHPdG and 8-OHdG.

**Table S4** Association between pathology and immunoscore of γ-OHPdG (Fisher test P=0.0364)

Sum score	Pathology					Total
	Normal	Cirrhosis with hyperplasia	Cirrhosis	Hyperplasia	HCC	
0	0	1	0	0	1	2
2	0	0	4	0	1	5
3	0	0	2	2	4	8
4	2	1	0	1	3	7
5	0	1	1	1	8	11
6	0	0	0	0	5	5
Total samples	2	3	7	4	22	38
Average score	4	3	2.7	3.8	4.4	

HCC, hepatocellular carcinoma.
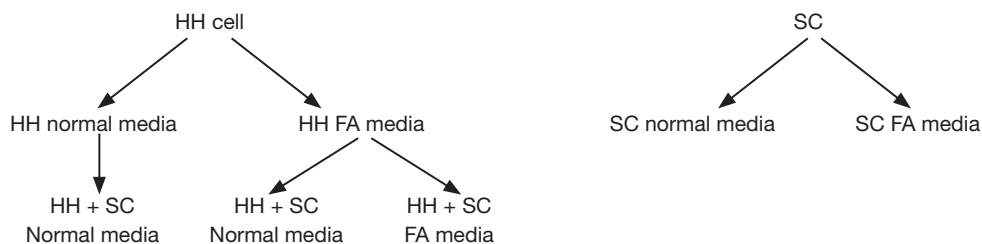

Figure S1 Diagram of experimental conditions.
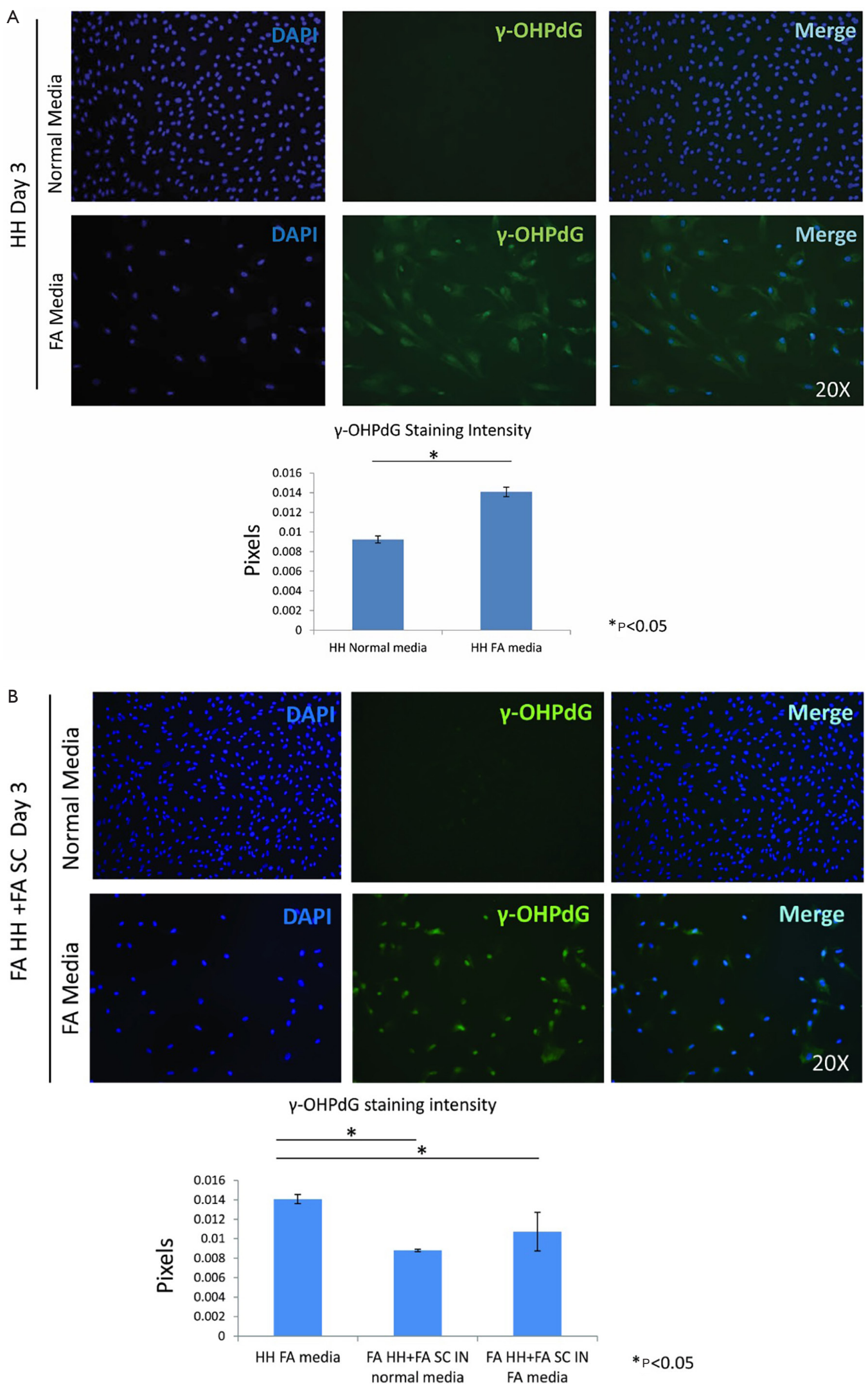
Figure S2 Co-culture in normal and FA conditions. (A) ICC and quantification of the ICC staining of γ-OHPdG of HH in normal media and FA media after 3 days; (B) fatty acid treated HH and SC in normal media by day 3 and FA-treated HH and FA SC in FA media by day 3 compared to HH in FA media with intensity quantification of γ-OHPdG. * indicates significance (P≤0.05) between groups using two-sample independent *t*-tests. ICC, immunocytochemistry; FA, fatty acids; HH, human hepatocytes.
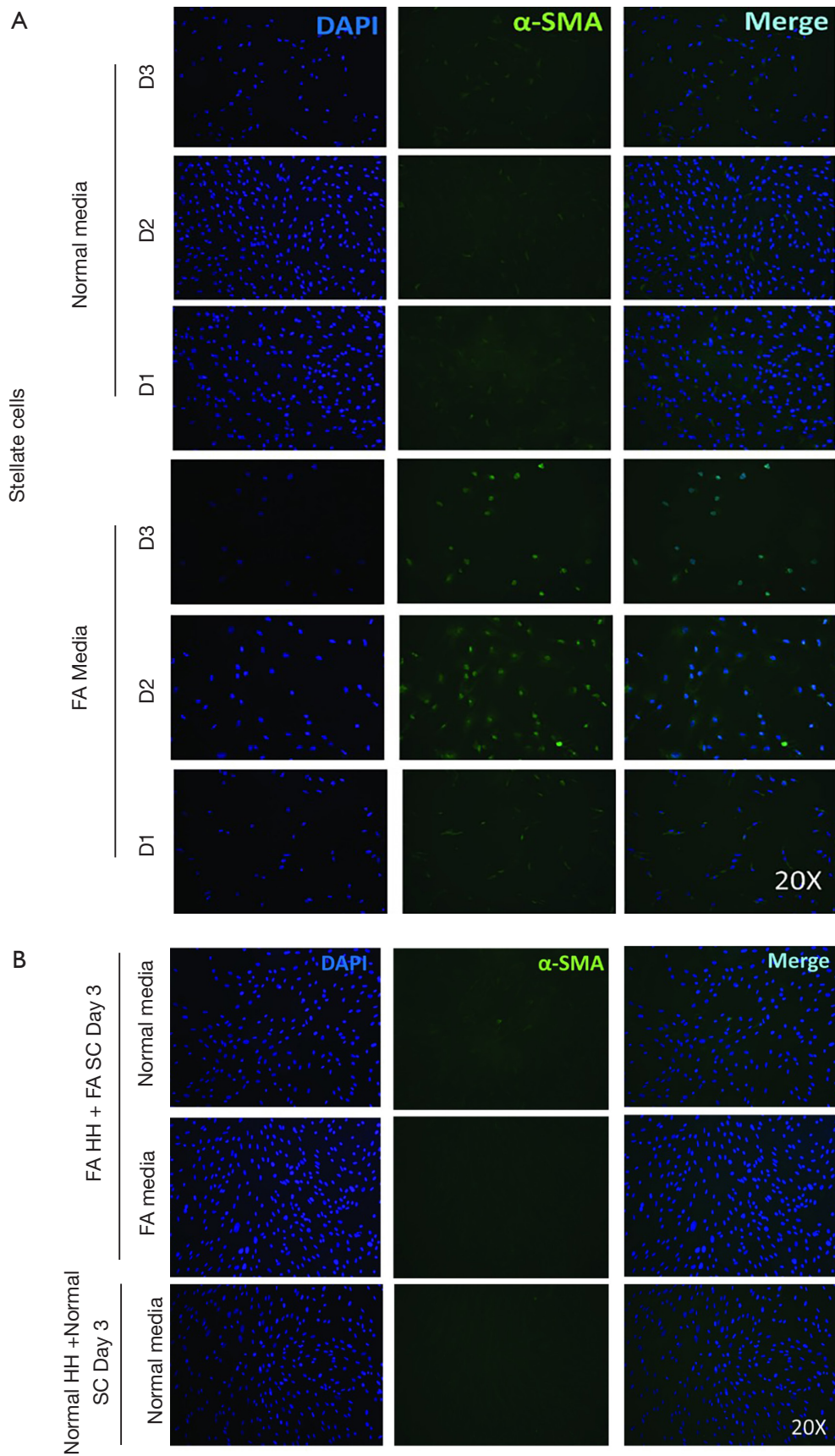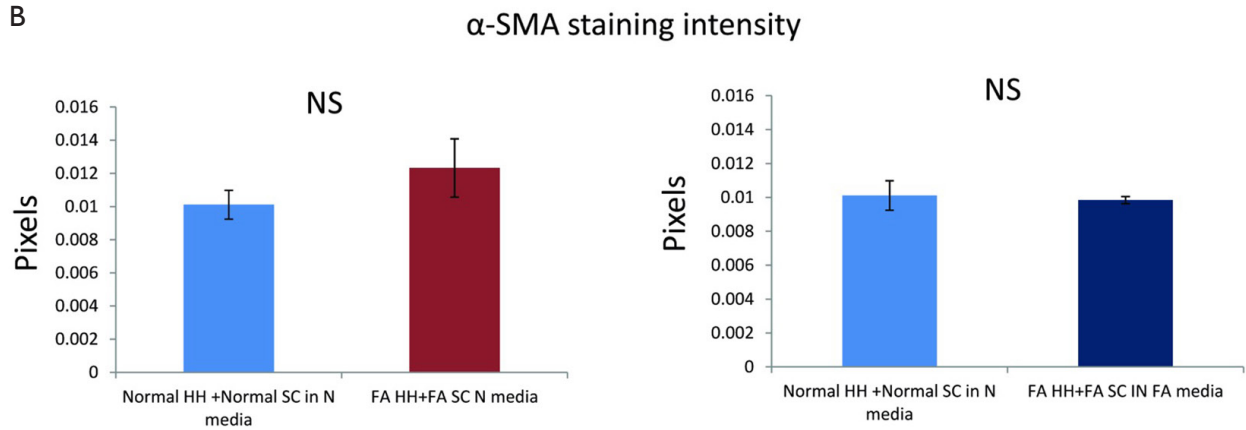
Figure S3 α-SMA staining in SC and HH co-culture. (A) FA HH co-cultured with FA SC in normal and FA media and normal HH co-cultured with normal SC in normal media by day 3; (B) SC in normal and FA media after 1, 3 and 5 days. HH, human hepatocytes; SC, stellate cell; α-SMA, alpha-smooth muscle actin.
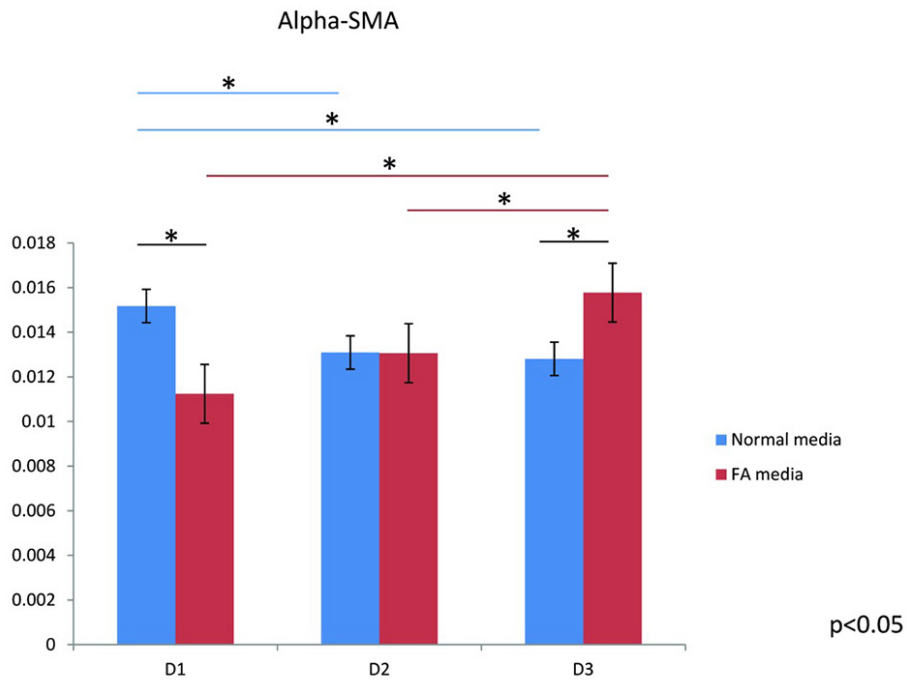
Figure S4 α-SMA staining of SC. (A,B) quantification of α-SMA intensity. SC, stellate cell; FA, fatty acids; α-SMA, alpha-smooth muscle actin.